HHS Public Access

Author manuscript

NMR Biomed. Author manuscript; available in PMC 2015 September 01.

Published in final edited form as:

NMR Biomed. 2014 September ; 27(9): 1135–1141. doi:10.1002/nbm.3167.

Field Dependence Study of *In Vivo* Brain ^{31}P MRS up to 16.4 Tesla

Ming Lu, **Wei Chen**, and **Xiao-Hong Zhu**[*]

Center for Magnetic Resonance Research, Department of Radiology, University of Minnesota Medical School, Minneapolis, Minnesota 55455, USA

Abstract

In vivo ^{31}P MRS provides a unique tool for studying bioenergetics of living organs. Although its utility has been limited by the relatively low ^{31}P NMR sensitivity, increasing magnetic field strength (B_0) could significantly improve the quality and reliability of the ^{31}P MR spectra for biomedical research. To quantitatively understand the field dependence of *in vivo* ^{31}P MRS for brain applications, ^{31}P NMR sensitivity of phosphocreatine (PCr) in rat brains was measured and compared at 9.4 T and 16.4 T. Additionally, the linewidths and T_1 relaxation times of PCr and adenosine triphosphate (ATP) resonances obtained from human and animal brains over a wide B_0 range from 4 T, 7 T, 9.4 T to 16.4 T were examined and their field dependences were quantified. The results indicate an approximate 1.74 fold ^{31}P signal-to-noise ratio (SNR) gain for PCr at 16.4 T compared to 9.4 T. An approximate power 1.4 dependence of ^{31}P SNR on B_0 was concluded. Substantial improvements in spectral resolution and significantly shortened T_1 values of brain PCr and ATP were observed at high/ultrahigh fields, contributing to an additional sensitivity gain and spectral improvement. In summary, the overall findings from this study suggest that *in vivo* ^{31}P MRS should greatly benefit from high/ultrahigh fields for noninvasive assessment of altered bioenergetics and metabolic processes associated with brain function and neurological diseases.

Keywords

^{31}P MRS; NMR sensitivity; linewidth; relaxation time; high/ultrahigh field

INTRODUCTION

In vivo ^{31}P magnetic resonance spectroscopy (MRS) enables direct measurement and quantification of high-energy phosphate (HEP) compounds such as adenosine triphosphate (ATP) and phosphocreatine (PCr), as well as inorganic phosphate (Pi) and other metabolites in the brain (1–3). These phosphorus metabolites are tightly coupled to the cerebral bioenergetics and their changes detected by *in vivo* ^{31}P MRS have been linked to numerous diseases, including brain ischemia (4), seizure, epilepsy (5,6), Alzheimer disease (7,8) and schizophrenia (9). When combined with magnetization transfer techniques, it is also possible to noninvasively measure the rates of ATP synthesis through the chemical exchange

[*]Correspondence to: Xiao-Hong Zhu, Ph.D., Center for Magnetic Resonance Research, Department of Radiology, University of Minnesota Medical School, 2012 6th Street S.E., Minneapolis, Minnesota 55455, USA, zhu@cmrr.umn.edu.

reactions involving creatine kinase and ATPase in the brain (10–17). Therefore, *in vivo* ^{31}P MRS provides a unique tool for directly investigating the synthesis, transfer, and utilization of high-energy phosphate compounds, which should significantly advance the understanding of bioenergetics associated with brain functions and disorders. In addition, other important and physiologically relevant information such as intracellular pH, free magnesium concentration, intermediates of phospholipid metabolism, and NAD^+/NADH redox states could also be obtained from brain ^{31}P spectra (2,18,19). However, *in vivo* ^{31}P MRS applications in biomedical research have faced a number of challenges including low concentration of phosphorus metabolites of interest, limited NMR sensitivity due to relatively low ^{31}P gyromagnetic ratio compared to that of ^{1}H, and limited spectral and spatial resolutions.

Previous studies have demonstrated that *in vivo* ^{31}P MRS can benefit from higher magnetic field strength (B_0) for overcoming the intrinsic sensitivity limitation and improving spectral resolution (20–23). However, the achievable signal-to-noise ratio (SNR) (24) of ^{31}P resonance measured in a fixed acquisition time depends not only on B_0 and its power term (defined as β and its value is expected to be in the range of 1–1.5 (25,26)), but also on many field-dependent parameters according to the following relationship (20,27):

$$\mathrm{SNR(in\ a\ fixed\ acquisition\ time)} \propto B_0^{\beta} Q^{1/2} \left(\frac{1}{T_1 \cdot \Delta\nu_{1/2}}\right)^{1/2} (1 - E_2^2)^{1/2} G(x) \quad [1]$$

where Q is the radiofrequency (RF) coil quality factor (under the sample loaded condition), T_1 is the longitudinal relaxation time, $\Delta\nu_{1/2}$ is the resonance linewidth at half peak height (in Hz, which is inversely proportional to the apparent transverse relaxation time (T_2^*)), $E_2^2 = e^{(-2 \cdot at \cdot \pi \cdot \Delta\nu_{1/2})}$ (*at* is the time for acquiring the ^{31}P free induction decay signal), and $G(x) = \left(2 \cdot \frac{1 - e^{-x}}{x(1+e^{-x})}\right)^{1/2}$ ($x = TR/T_1$ and *TR* is the repetition time) (20,25–27). Therefore, in order to evaluate the quantitative relationship between the field strength and the sensitivity of the *in vivo* brain ^{31}P MRS as defined by the SNR per fixed acquisition time, it is necessary to consider all relevant field-dependent and acquisition parameters as expressed in Equation [1] at different fields.

It is known that resonance linewidth (in Hz unit) broadens with increasing B_0, which could reduce the SNR and affect the spectral resolution. Thus, the field dependence of the resonance linewidth is another key factor in determining the improvement of *in vivo* ^{31}P MR spectral quality at higher field. Moreover, for phosphorus metabolites such as ATP and PCr, both dipole-dipole interactions and chemical shift anisotropy (CSA) contribute to the T_1 relaxation processes, and their relative contributions depend on B_0 and the molecular structure (28). At high/ultrahigh field, the CSA contribution to T_1 relaxation ($T_{1(CSA)}$) can become dominant due to the dependence of $1/T_{1(CSA)}$ on the square power of B_0 (29,30), thus shortening the ^{31}P T_1 values of ATP and PCr.

To quantitatively understand the field-dependence of *in vivo* ^{31}P MRS, the following experiments were designed and conducted. Firstly, the ^{31}P NMR sensitivity of the PCr

signal was compared in rat brains at the ultrahigh fields of 9.4 T and 16.4 T with identical experimental setups. Secondly, the resonance linewidths (in Hz units) and spectral resolutions (in ppm units) of PCr, α-ATP, and γ-ATP resonances obtained from human and animal brains covering a wide B_0 range up to 16.4 T were quantitatively compared to determine their field dependences. Thirdly, the field dependence of the PCr and ATP T_1 relaxation times in human and animal brains was investigated. Finally, the quantitative relationships between the SNR of the PCr and ATP resonances and the B_0 from 4 T to 16.4 T were deduced based on the experimental results of multiple field-dependent parameters.

Instead of investigating and predicting the theoretical field-dependence of intrinsic SNR and natural linewidth, the purpose of this study was to understand the practically achievable SNR and spectral resolution at a given field strength and their relative improvements with increasing B_0 field, since this information is most relevant to the majority of *in vivo* ^{31}P MRS brain applications.

METHODS

Comparison study of *in vivo* ^{31}P MRS sensitivity at 9.4 T and 16.4 T

The *in vivo* ^{31}P SNR comparison study was conducted on 9.4 T/31 cm bore and 16.4 T/26 cm bore magnets (Magnex Scientific) interfaced to VNMRJ consoles from the same vendor (Agilent, CA). Passively decoupled dual-coil RF probes with identical geometry were constructed for 9.4 T and 16.4 T experiments and placed over the rat brains to obtain optimum detection sensitivity. Each probe consisted of a one-turn, oval (14 mm × 20 mm) shaped single-loop ^{31}P surface coil for ^{31}P MRS and a butterfly ^{1}H surface coil (28 mm × 20 mm) for shimming and anatomical images.

Male Sprague Dawley rats were anesthetized with 2% (v/v) isoflurane in a mixture of O_2 and N_2O gases (~2:3), and scanned at 9.4 T and 16.4 T (five rats for each field strength). All animal procedures for rat preparation, anesthesia, and maintenance under physiological conditions during the measurements were the same as described in a previous report (31).

A single-pulse-acquisition sequence was applied to obtain the brain ^{31}P signal and to calibrate the nominal 90° of the RF excitation pulse (where a maximum ^{31}P signal was approached) with the following acquisition parameters: 200μs hard pulse, 8 kHz spectral width (SW), 1024 number of points (NP) for each free induction decay (FID), 10 s repetition time (TR) and 8 signal averages (NT). The raw ^{31}P MRS signal was processed by exponential filtering with a line broadening (LB) of 20 Hz to enhance apparent SNR, followed by Fourier transformation. The ^{31}P NMR sensitivity was evaluated using the SNR of the PCr resonance calculated by dividing the PCr resonance height by the peak-to-peak spectral noise, and multiplying it by 2.5 to minimize the errors of noise measurement caused by spectral baseline drifting (20,31–33).

Practically, several factors, which are not included in Equation [1], can also influence the SNR values measured at different fields, and their possible confounding effects were carefully considered when conducting the SNR comparison study at 9.4 T and 16.4 T. For example, the same RF coil size and geometry, same pulse flip angle, as well as the same

position between the coil and rat head were used to ensure identical RF excitation and reception profiles at these two fields. In addition, the same acquisition parameters including the spectral width were applied, and a similar receiver noise figure was confirmed at 9.4T and 16.4T.

In vivo ^{31}P MRS studies of field dependence of PCr and ATP linewidths and spectral resolution

For studying the field dependence of PCr and ATP resonance linewidths and spectral resolution, *in vivo* ^{31}P spectra were acquired from either human brains at 4 T/90 cm bore (Oxford) and 7 T/90 cm bore (Magnex Scientific) magnets interfaced with Varian consoles (Agilent, CA), or cat brains at 9.4 T and 16.4 T. Nine healthy human adults (19–50 years old; four for 4 T and five for 7 T) and eight adolescent cats (weight 0.8–1.6 kg; four for 9.4 T and another four for 16.4 T) were used. More information about cat preparation and maintenance can be found in a previous report (34).

A set of home-built and passively decoupled ^{31}P/^{1}H RF dual surface coils were applied to collect the ^{31}P signals with a single-pulse-acquisition sequence, without the use of ^{1}H decoupling, from the human and cat visual cortices at various field strengths of 4 T, 7 T, 9.4 T and 16.4 T. B_0 field homogeneity was achieved by shimming the water ^{1}H resonance of the occipital brain region using the FASTMAP algorithm (35). A relatively long repetition time (TR: 3–16 s) and a high signal average (NT: 40–320) were used for achieving sufficient SNR. All ^{31}P spectra were processed without a line broadening before Fourier transformation to measure resonance linewidths. The resonance linewidths of PCr, γ-ATP, and α-ATP at half peak height were regressed and quantified for each spectrum acquired at different magnetic field strengths using the VNMRJ software package. The linewidth results of 1.5 T and 2 T taken from the literature (21) were also included in this study to further extend the B_0 range for comparison.

Since the outcome of linewidth measurements is subject to the quality of shimming, it is essential to optimize the B_0 homogeneity within the sample volume covered by the ^{31}P RF coil. Extra cautions were taken in this study to minimize the possible confounding effect due to shimming variation. For instance, ^{31}P linewidths were measured from the visual cortex of human and cat, which approximates a spherical shape favorable for optimal shimming; the ^{31}P RF coil sizes (5 cm diameter for human and oval shaped 1.4 cm × 2 cm for cat) were optimized to ensure that the ^{31}P signals were mainly detected from the visual cortex with negligible muscle contribution. Also, both first and second-order FASTMAP shimming (35) was applied for further improving the B_0 homogeneity and the resonance linewidths.

In vivo measurements of PCr and ATP T_1 relaxation times at different fields

The T_1 values of PCr in rat brains at both 9.4 T and 16.4 T (four rats for each field strength) were measured using an inversion recovery pulse sequence under the fully relaxed condition with a long pre-inversion delay (d1) of 16 s with 8 signal averages. A B_1-insensitive hyperbolic secant inversion pulse (36,37) was used to compensate the B_1 inhomogeneity of the ^{31}P surface coil followed by magnetization dephasing gradients. T_1 values were

determined by a three-parameter least-square fitting of a single exponential function to the PCr signals with a total of nine different inversion times (TI: 0.012–20 s) at each field.

Similarly, the T_1 values of PCr, γ-ATP, and α-ATP were also determined in the cat visual cortex at 9.4T (seven cats with d1 of 20 s and 12–16 signal averages, TI: 0.08–20.48 s) and 16.4T (six cats with d1 of 16 s and 16–24 signal averages, TI: 0.012–20 s), and in the human visual cortex at 4T (twelve subjects with d1 of 16 s and 16 signal averages, TI: 0.025–32 s) and 7T (ten subjects with d1 of 16 s and 8–12 signal averages, TI: 0.008–20 s).

The experimental procedures of human studies were approved by the Institutional Review Board of the University of Minnesota with written informed consent obtained from all subjects prior to study. The Institutional Animal Care and Use Committee of the University of Minnesota approved the animal procedures and experimental protocols.

All results presented in this study are shown as mean standard deviation.

RESULTS

The averaged PCr ^{31}P SNR obtained at 16.4 T was 1.74 fold higher than that at 9.4 T for the rat brains, as shown in Table 1. Similar SNR improvements were also observed in a phantom solution containing Pi and from localized *in vivo* ^{31}P spectra of the rat brains measured at these two fields (data not shown herein). The overall results demonstrate an excellent sensitivity at both high fields for obtaining ^{31}P signals; nevertheless, the 16.4 T scanner offers a remarkable improvement in the ^{31}P NMR sensitivity.

Figure 1 displays typical *in vivo* ^{31}P spectra obtained either from human visual cortex at 4 T (Fig. 1a) and 7 T (Fig. 1b) or from cat visual cortex at 9.4 T (Fig. 1c) and 16.4 T (Fig. 1d). It clearly indicates that the linewidths of metabolite resonances in ppm scale reduced substantially when the field strength was increased from 4 T to 16.4 T, thus significantly improving the spectral resolution and the separation of adjacent resonances. The linewidth dependences of three major high-energy phosphate resonances (PCr, γ-ATP, and α-ATP) on B_0 from the human and cat brains are shown in Fig. 2. When using Hz as the unit of linewidth, linear correlations according to the following regressed equations were observed for all resonances studied (Fig. 2a):

$$\Delta\nu_{1/2,\mathrm{PCr}}=0.41\mathrm{B}_0+10.6,\quad \mathrm{R}^2=0.50 \quad [2a]$$

$$\Delta\nu_{1/2,\alpha-\mathrm{ATP}}=1.45\mathrm{B}_0+28.7,\quad \mathrm{R}^2=0.99 \quad [2b]$$

$$\Delta\nu_{1/2,\gamma-\mathrm{ATP}}=3.02\mathrm{B}_0+22.3,\quad \mathrm{R}^2=0.99 \quad [2c]$$

However, such linear correlations between linewidth and B_0 became approximately inverse relationships when the unit of the linewidth was converted from Hz to ppm as shown in Fig. 2b, indicating a drastic improvement in ^{31}P spectral resolution at high/ultrahigh fields.

Figure 2c illustrates the exponential fittings of the *in vivo* ^{31}P signals as a function of the inversion times at either 9.4 T or 16.4 T for the T_1 measurements of PCr in the rat brain. The measured PCr T_1 values were 2.95 ± 0.11 s (N = 4) and 1.56 ± 0.05 s (N = 4) for 9.4 T and 16.4 T, respectively. For the T_1 comparisons between different species, PCr T_1 values of cat brains were also measured at 9.4 T (T_1 = 2.60 ± 0.07 s; N = 7) and 16.4 T (T_1 = 1.50 ± 0.03 s; N = 6). The slightly longer T_1 values of PCr in the rat brains could be due to partial signal contribution from surrounding muscle. To extend the B_0 range, T_1 values of PCr from human brains at 4 T (T_1 = 4.36 ± 0.25 s; N = 12) and 7 T (T_1 = 3.54 ± 0.21 s; N = 10) were also included and compared in this study. Figure 2d shows an approximately exponential decay dependence of PCr T_1 values on the field strength between 4 T and 16.4 T according to the following regressed equation with an excellent regression coefficient:

$$T_{1,PCr}=6.248\cdot e^{-0.086\cdot B_0} \quad R^2=0.99 \quad [3a]$$

Similar dependences were also observed for α-ATP and γ-ATP (data and regression curves are not shown herein) across a wide B_0 range from 4T to 16.4T:

$$T_{1,\alpha-ATP}=1.846\cdot e^{-0.073\cdot B_0} \quad R^2=1.00 \quad [3b]$$

$$T_{1,\gamma-ATP}=1.754\cdot e^{-0.046\cdot B_0} \quad R^2=0.99 \quad [3c]$$

When applying all field-dependent parameters obtained from rat brain at 9.4 T and 16.4 T (including the values of $\Delta\nu_{1/2}$, Q, T_1, *at*, TR, E_2^2 and G(x) as summarized in Table 1) into Equation [1], a power (β) dependence of PCr SNR on B_0 of approximately 1.42 was deduced using Equation [4],

$$\frac{SNR_{16.4T}}{SNR_{9.4T}}=1.74=(B_0\text{ratio})^{\beta}\sqrt{Q\text{ratio}}\sqrt{\frac{1}{T_1\text{ratio}}}\sqrt{\frac{1}{\Delta\nu_{1/2}\text{ratio}}}\times(G\text{ratio})=\left(\frac{16.4}{9.4}\right)^{\beta}\sqrt{0.873}\sqrt{\frac{1}{0.529}}\sqrt{\frac{1}{1.505}}\times 0.757 \quad [4]$$

This result is in excellent agreement with the theoretical prediction of β=1.5 when the coil noise is dominate (25,26), and with the comparison result of human brain at 4 T and 7 T (β=1.4) as previously reported (20).

Equation [1] can be further simplified using the key parameters that are sensitive to B_0 to estimate the SNR ratio (R_{SNR}) at higher field relative to 4 T, while term E_2^2 (≈ 0 for most cases) can be omitted:

$$R_{SNR}=\left(\frac{B_0}{4}\right)^{1.5}\left(\frac{Q}{Q_{4T}}\right)^{\frac{1}{2}}\sqrt{\frac{T_{1,4T}\cdot\Delta\nu_{1/2,4T}}{T_1\cdot\Delta\nu_{1/2}}}\left(\frac{G(x)}{G(x)_{4T}}\right)=\sqrt{\frac{Q}{Q_{4T}}}\left(\frac{G(x)}{G(x)_{4T}}\right)\cdot R'_{SNR} \quad [5]$$

and

$$R'_{SNR} = \left(\frac{B_0}{4}\right)^{1.5} \sqrt{\frac{T_{1,4T} \cdot \Delta\nu_{1/2,4T}}{T_1 \cdot \Delta\nu_{1/2}}} \quad [6]$$

In Equation [5], the relative SNR contribution from the G(x) term depends on the TR and T_1 values, and it is close to 1 for most *in vivo* ^{31}P MRS applications with a TR/T_1 ratio of < 1 (20), although it was offset from 1 in this study due to the application of a much longer TR (Table 1). Nevertheless, the SNR contribution of the G term can be readily calculated if the T_1 and TR values are known. There is not a simple way, however, to provide *a priori* estimation of the relative SNR contribution from the Q term since it is difficult to predict the loaded Q value of a particular RF coil at a given field strength. The Q value of a RF coil depends on many factors including its operating Larmor frequency, coil geometry and size, the sample size and loading property, etc., and it has to be determined experimentally under the sample loaded conditions. Therefore, based on the field dependent relationships (i.e., Eqs. [2] and [3]) deduced in the present study), Equation [6] was used to estimate the relative SNR improvement at higher fields to that of 4T. As a result, Figure 3 quantitatively shows the contributions from the B_0, T_1, and $\Delta\nu_{1/2}$ terms (either individual or combined effect) to the ^{31}P SNR gain for PCr, α-ATP, and γ-ATP resonances, at high/ultrahigh fields.

DISCUSSION AND CONCLUSION

In this study, we first examined and compared the ^{31}P NMR sensitivity in rat brain between 9.4 T and 16.4 T. The results show an approximately 1.74 fold ^{31}P SNR gain at 16.4 T compared to that at 9.4 T, which is consistent with the previous ^{31}P MR sensitivity comparison study in human brain at 7T vs. 4T (20). The T_1 relaxation times of PCr in rat brains at these two fields were also measured and a 47% decrease of PCr T_1 value was observed at 16.4T. Similar reductions in T_1 relaxation times of PCr and ATP were also observed in the cat and human brains across a wide range of B_0 from 4 T to 16.4 T as summarized in Fig. 2d and Equation [3]. Such field dependences of T_1 are presumably due to the fact that the CSA rather than the dipole-dipole interaction mechanism dominants the relaxation process of these phosphorus metabolites at high/ultrahigh field (28–30). This phenomenon is different from that observed in MRI, in which the ^{1}H T_1 of the tissue water has been found to increase with magnetic field strength since the proton relaxation is dominated by the dipole-dipole interaction mechanism. The shortened T_1 values of PCr and ATP resonances at higher field would allow more signal averaging within the same acquisition time, thus increasing the achievable SNR of ^{31}P MRS. These findings indicate that increasing field strength not only significantly improves the *in vivo* ^{31}P MRS detection sensitivity and quality, but also can shorten the total acquisition time for acquiring localized ^{31}P MRS or three-dimensional imaging which usually requires a large number of k-space samples.

Another topic of interest in this study was the field dependence of PCr and ATP linewidths. Figures 2a and 2b summarize the field-dependent relationships of brain PCr and ATP linewidths across a very wide B_0 range from 1.5 T to 16.4 T. In general, all linewidths in Hz unit were positively correlated to B_0 with high linearity and very small error bars (Fig. 2a).

However, the regression slopes were substantially different between different resonances, showing the smallest slope for PCr and largest slope for γ-ATP as described by Eq. [2]. Interestingly, the slope of γ-ATP was two times higher than that of α-ATP for the two phosphate spins within the same ATP molecule, and the two lines intersected at about 4 T where α-ATP and γ-ATP had equal linewidths (see Fig. 2a). These results suggest distinct relaxation behaviors between α-ATP and γ-ATP, which may reflect their different spin environments. As expected, we also observed that the intercepts for both γ-ATP and α-ATP lines at zero field strength were larger than that of the ^{31}P-^{31}P J-coupling constant (about 20 Hz). Both γ-ATP and α-ATP resonances are doublets separated by the ^{31}P-^{31}P J-coupling constant. The linewidths measured in this study are the apparent linewidths of the ATP resonances including the broadening effect caused by the ^{31}P-^{31}P J-coupling splitting. Nevertheless, the linewidths of their single resonances can be determined by subtracting the ^{31}P-^{31}P J-coupling constant from the apparent linewidth values (in Hz, as shown in Fig. 2a or summarized by Eqs. [2b] and [2c]). Importantly, the rates of the linewidth broadening (in the unit of Hz) as a function of B_0 were much slower than that of B_0 increasing for all resonances studied, e.g., increasing B_0 from 4 T to 16.4 T (> 4 times) only approximately doubles the linewidth for γ-ATP. Therefore, the "true" ^{31}P spectral resolution (i.e., the linewidths in the ppm scale as demonstrated in Figs. 1 and 2b,) is significantly improved at high/ultrahigh fields, especially in the B_0 range of 1.5 T towards 9.4 T.

To understand the relative improvement of the ^{31}P SNR that is *practically achievable* at a given field strength as compare to that of 4T, Eq. [5] has been derived to account for the contributions from all B_0 dependent parameters shown in Eq. [1]. If the contributions from the experimentally specific terms such as Q and G(x), which need to be determined based on the actual coil and acquisition conditions used in a particular study, are excluded, then Eq. [6] can be used to estimate the apparent SNR ratio at high/ultrahigh fields relative to 4T. As a summary, Fig. 3 displays the SNR gains for the brain PCr, α-ATP and γ-ATP resonances at high/ultrahigh fields (> 4 T) due to the contributions from B_0, T_1, and/or $\Delta\nu_{1/2}$. The most significant SNR gain is from the increasing magnetic field strength with the β power of 1.4–1.5 (dashed lines in Fig. 3d–3f); the sample loading and the operating frequency of the RF coil will affect the actual value of the β power (25,26). The consistent β values of approximate 1.4 as observed in the rat brain and the human occipital cortex *in vivo* using surface coils suggest that the coil noise likely dominated the noise contribution to the measured SNR. In contrast, for a volume RF coil with a heavy sample loading (e.g., human head) or a large RF coil operated at very high frequency, the increasing sample noise contribution will reduce the SNR gain at higher fields and reduce the β value below 1.5 when the sample noise becomes dominant (25).

It is also worth noting that identical spectral widths (SW=8kHz) were applied in the present SNR comparison study of rat brain between 9.4T and 16.4T to exclude the confounding effect of SW on the overall SNR (inversely proportional to square root of SW). However, practically, the optimal SW at lower fields for covering the same chemical shift range (in ppm unit) can be reduced as compared to higher fields, which will slightly negate the SNR benefit at higher field.

The broadened lines ($\Delta\nu_{1/2}$) at higher fields could lead to a reduction in signal intensity (dashed lines in Fig.3a–3c), and thus a SNR loss. This loss, however, could be compensated completely (for the PCr and α-ATP resonances) or partially (for γ-ATP resonance) by the shortened T_1 values. As a result, the net effect of combined T_1 and $\Delta\nu_{1/2}$ contributions leads to a significant SNR enhancement of >40% for PCr and >20% for α-ATP at 16.4 T as compared to 4 T, or a small SNR loss of <5% for the γ-ATP resonance (solid lines in Fig. 3a–3c). It has been reported that, in a solution at 37°C, the relative contribution of CSA increases from 14% at 2.3T to 59% at 7T for α-ATP, in contrast to a lesser degree of increase for γ-ATP from 5% at 2.3T to 34% at 7T (28), indicating a stronger CSA effect for ±-ATP than γ-ATP at higher field. This finding on the field-dependent ^{31}P CSA is consistent with the *in vivo* results of the present study, in which a relatively slower decay of γ-ATP T_1 with increasing B_0 (Eq. [3c]) was observed as compared to that of α-ATP (Eq. [3b]). Nevertheless, all three HEP resonances benefit significantly from increased magnetic field strength in terms of overall SNR gain and spectral resolution improvement as quantitatively illustrated in Figs. 2 and 3. Finally, the findings of the present work suggest that a comprehensive approach based on Eqs. [1] and [5] or [6] can be applied to robustly quantify the achievable SNR gain of *in vivo* ^{31}P MRS for brain applications at different fields as demonstrated herein.

In conclusion, the overall results of this study quantitatively demonstrate the substantial sensitivity and quality improvements of *in vivo* ^{31}P brain MRS at high/ultrahigh fields. Such improvements should greatly benefit many biomedical applications of *in vivo* ^{31}P MRS in assessing altered bioenergetics and metabolic processes associated with brain function and neurological diseases.

ACKNOWLEDGEMENTS

The authors would like to thank Professor Kamil Ugurbil for his support and Drs. Fei Du, Hongyang Qiao and Yi Zhang for assistance in data collection and/or animal preparation.

Grant Sponsor: National Institute of Health; Grant numbers: NS041262, NS057560, NS070839, P41 RR008079, P41 EB015894 and P30 NS057091, S10 RR025031; and the Keck foundation.

Abbreviations

MRS	magnetic resonance spectroscopy
MRSI	magnetic resonance spectroscopy imaging
NMR	nuclear magnetic resonance
B_0	magnetic field strength
HEP	high-energy phosphate
Pi	inorganic phosphate
PCr	phosphocreatine
ATP	adenosine triphosphate
SNR	signal-to-noise ratio

T_1	longitudinal relaxation time
T_2^*	apparent transverse relaxation time
$\Delta\nu_{1/2}$	resonance linewidth at half peak height
RF	radiofrequency
Q	radiofrequency coil quality factor
CSA	chemical shift anisotropy

REFERENCES

1. Ackerman JJ, Grove TH, Wong GG, Gadian DG, Radda GK. Mapping of metabolites in whole animals by ^{31}P NMR using surface coils. Nature. 1980; 283:167–170. [PubMed: 7350541]
2. Lei H, Zhu XH, Zhang XL, Ugurbil K, Chen W. In vivo ^{31}P magnetic resonance spectroscopy of human brain at 7 T: an initial experience. Magnetic resonance in medicine. 2003; 49:199–205. [PubMed: 12541238]
3. Shulman RG, Brown TR, Ugurbil K, Ogawa S, Cohen SM, den Hollander JA. Cellular applications of ^{31}P and ^{13}C nuclear magnetic resonance. Science. 1979; 205:160–166. [PubMed: 36664]
4. Welch KM, Levine SR, Martin G, Ordidge R, Vande Linde AM, Helpern JA. Magnetic resonance spectroscopy in cerebral ischemia. Neurol Clin. 1992; 10:1–29. [PubMed: 1556996]
5. Hetherington HP, Pan JW, Spencer DD. ^{1}H and ^{31}P spectroscopy and bioenergetics in the lateralization of seizures in temporal lobe epilepsy. J Magn Reson Imaging. 2002; 16:477–483. [PubMed: 12353261]
6. Weiner MW. NMR spectroscopy for clinical medicine. Animal models and clinical examples. Ann N Y Acad Sci. 1987; 508:287–299. [PubMed: 3326457]
7. Brown GG, Levine SR, Gorell JM, Pettegrew JW, Gdowski JW, Bueri JA, Helpern JA, Welch KM. In vivo ^{31}P NMR profiles of Alzheimer's disease and multiple subcortical infarct dementia. Neurology. 1989; 39:1423–1427. [PubMed: 2812317]
8. Bottomley PA, Cousins JP, Pendrey DL, Wagle WA, Hardy CJ, Eames FA, McCaffrey RJ, Thompson DA. Alzheimer dementia: quantification of energy metabolism and mobile phosphoesters with P-31 NMR spectroscopy. Radiology. 1992; 183:695–699. [PubMed: 1584923]
9. Pettegrew JW, Minshew NJ. Molecular insights into schizophrenia. J Neural Transm Suppl. 1992; 36:23–40. [PubMed: 1527518]
10. Zhu XH, Du F, Zhang N, Zhang Y, Lei H, Zhang X, Qiao H, Ugurbil K, Chen W. Advanced In vivo heteronuclear MRS approaches for studying brain bioenergetics driven by mitochondria. Methods Mol Biol. 2009; 489:317–357. [PubMed: 18839099]
11. Alger JR, Shulman RG. NMR studies of enzymatic rates in vitro and in vivo by magnetization transfer. Q Rev Biophys. 1984; 17:83–124. [PubMed: 6091170]
12. Du F, Zhu XH, Qiao H, Zhang X, Chen W. Efficient in vivo ^{31}P magnetization transfer approach for noninvasively determining multiple kinetic parameters and metabolic fluxes of ATP metabolism in the human brain. Magnetic resonance in medicine. 2007; 57:103–114. [PubMed: 17191226]
13. Du F, Zhu XH, Zhang Y, Friedman M, Zhang N, Ugurbil K, Chen W. Tightly coupled brain activity and cerebral ATP metabolic rate. Proc Natl Acad Sci U S A. 2008; 105:6409–6414. [PubMed: 18443293]
14. Lei H, Ugurbil K, Chen W. Measurement of unidirectional Pi to ATP flux in human visual cortex at 7 T by using in vivo ^{31}P magnetic resonance spectroscopy. Proc Natl Acad Sci U S A. 2003; 100:14409–14414. [PubMed: 14612566]
15. Shoubridge EA, Briggs RW, Radda GK. ^{31}p NMR saturation transfer measurements of the steady state rates of creatine kinase and ATP synthetase in the rat brain. FEBS letters. 1982; 140:289–292. [PubMed: 6282642]

16. Bottomley PA, Hardy CJ. Mapping creatine kinase reaction rates in human brain and heart with 4 Tesla saturation transfer ^{31}P NMR. J Magn Reson. 1992; 99:443–448.
17. Xiong Q, Du F, Zhu XH, Zhang P, Suntharalingam P, Ippolito J, Kamdar FD, Chen W, Zhang J. ATP production rate via creatine kinase or ATP synthase in vivo: a novel superfast magnetization saturation transfer method. Circ Res. 2011; 108:653–663. [PubMed: 21293002]
18. Keshavan MS, Stanley JA, Montrose DM, Minshew NJ, Pettegrew JW. Prefrontal membrane phospholipid metabolism of child and adolescent offspring at risk for schizophrenia or schizoaffective disorder: an in vivo ^{31}P MRS study. Mol Psychiatry. 2003; 8:316–323. 251. [PubMed: 12660804]
19. Lu M, Zhu XH, Zhang Y, Chen W. Intracellular redox state revealed by in vivo ^{31}P MRS measurement of NAD^+ and NADH contents in brains. Magnetic resonance in medicine. 2014; 71:1959–1972. [PubMed: 23843330]
20. Qiao HY, Zhang XL, Zhu XH, Du F, Chen W. In vivo ^{31}P MRS of human brain at high/ultrahigh fields: a quantitative comparison of NMR detection sensitivity and spectral resolution between 4 T and 7 T. Magnetic resonance imaging. 2006; 24:1281–1286. [PubMed: 17145398]
21. Boska MD, Hubesch B, Meyerhoff DJ, Twieg DB, Karczmar GS, Matson GB, Weiner MW. Comparison of ^{31}P MRS and ^{1}H MRI at 1.5 and 2.0 T. Magnetic resonance in medicine. 1990; 13:228–238. [PubMed: 2314213]
22. Hardy CJ, Bottomley PA, Roemer PB, Redington RW. Rapid ^{31}P spectroscopy on a 4-T whole-body system. Magnetic resonance in medicine. 1988; 8:104–109. [PubMed: 3173064]
23. Hetherington HP, Spencer DD, Vaughan JT, Pan JW. Quantitative ^{3}1P spectroscopic imaging of human brain at 4 Tesla: assessment of gray and white matter differences of phosphocreatine and ATP. Magnetic resonance in medicine. 2001; 45:46–52. [PubMed: 11146485]
24. Redpath TW, Wiggins CJ. Estimating achievable signal-to-noise ratios of MRI transmit-receive coils from radiofrequency power measurements: applications in quality control. Physics in medicine and biology. 2000; 45:217–227. [PubMed: 10661593]
25. Hoult DI, Lauterbur PC. The sensitivity of the zeugmatographic experiment involving human samples. J Magn Reson. 1979; 34:425–433.
26. Hoult DI, Richards RE. Signal-to-noise ratio of nuclear magnetic resonance experiment. J Magn Reson. 1976; 24:71–85.
27. Ernst, RR.; Bodenhausen, G.; Wokaun, A. Principles of Nuclear Magnetic Resonance in One and Two Dimensions. New York: Oxford University Press; 1991.
28. Andrew ER, Gaspar R. Mechanisms of 31P relaxation in phosphorus metabolites. MAGMA. 1994; 2:421–423.
29. Evelhoch JL, Ewy CS, Siegfried BA, Ackerman JJ, Rice DW, Briggs RW. ^{31}P spin-lattice relaxation times and resonance linewidths of rat tissue in vivo: dependence upon the static magnetic field strength. Magnetic resonance in medicine. 1985; 2:410–417. [PubMed: 4094555]
30. Mathur-De Vre R, Maerschalk C, Delporte C. Spin-lattice relaxation times and nuclear Overhauser enhancement effect for ^{31}P metabolites in model solutions at two frequencies: implications for in vivo spectroscopy. Magnetic resonance imaging. 1990; 8:691–698. [PubMed: 2266794]
31. Lu M, Zhang Y, Ugurbil K, Chen W, Zhu XH. In vitro and in vivo studies of ^{17}O NMR sensitivity at 9.4 and 16.4 T. Magnetic resonance in medicine. 2013; 69:1523–1527. [PubMed: 22777729]
32. Zhu XH, Merkle H, Kwag JH, Ugurbil K, Chen W. ^{17}O relaxation time and NMR sensitivity of cerebral water and their field dependence. Magnetic resonance in medicine. 2001; 45:543–549. [PubMed: 11283979]
33. Martin, ML.; Martin, GJ.; Delpuech, JJ. Practical NMR Spectroscopy. London, UK: Heyden & Son Ltd; 1980.
34. Zhu XH, Zhang N, Zhang Y, Ugurbil K, Chen W. New insights into central roles of cerebral oxygen metabolism in the resting and stimulus-evoked brain. J Cereb Blood Flow Metab. 2009; 29:10–18. [PubMed: 18781163]
35. Gruetter R. Automatic, localized in vivo adjustment of all first- and second-order shim coils. Magnetic resonance in medicine. 1993; 29:804–811. [PubMed: 8350724]
36. Baum J, Tycko R, Pines A. Broad-band and adiabatic inversion of a 2-level system by phase-modulated pulses. Phys Rev A. 1985; 32:3435–3447. [PubMed: 9896511]

37. Silver MS, Joseph RI, Hoult DI. Highly selective Pi/2 and Pi-pulse generation. J Magn Reson. 1984; 59:347–351.

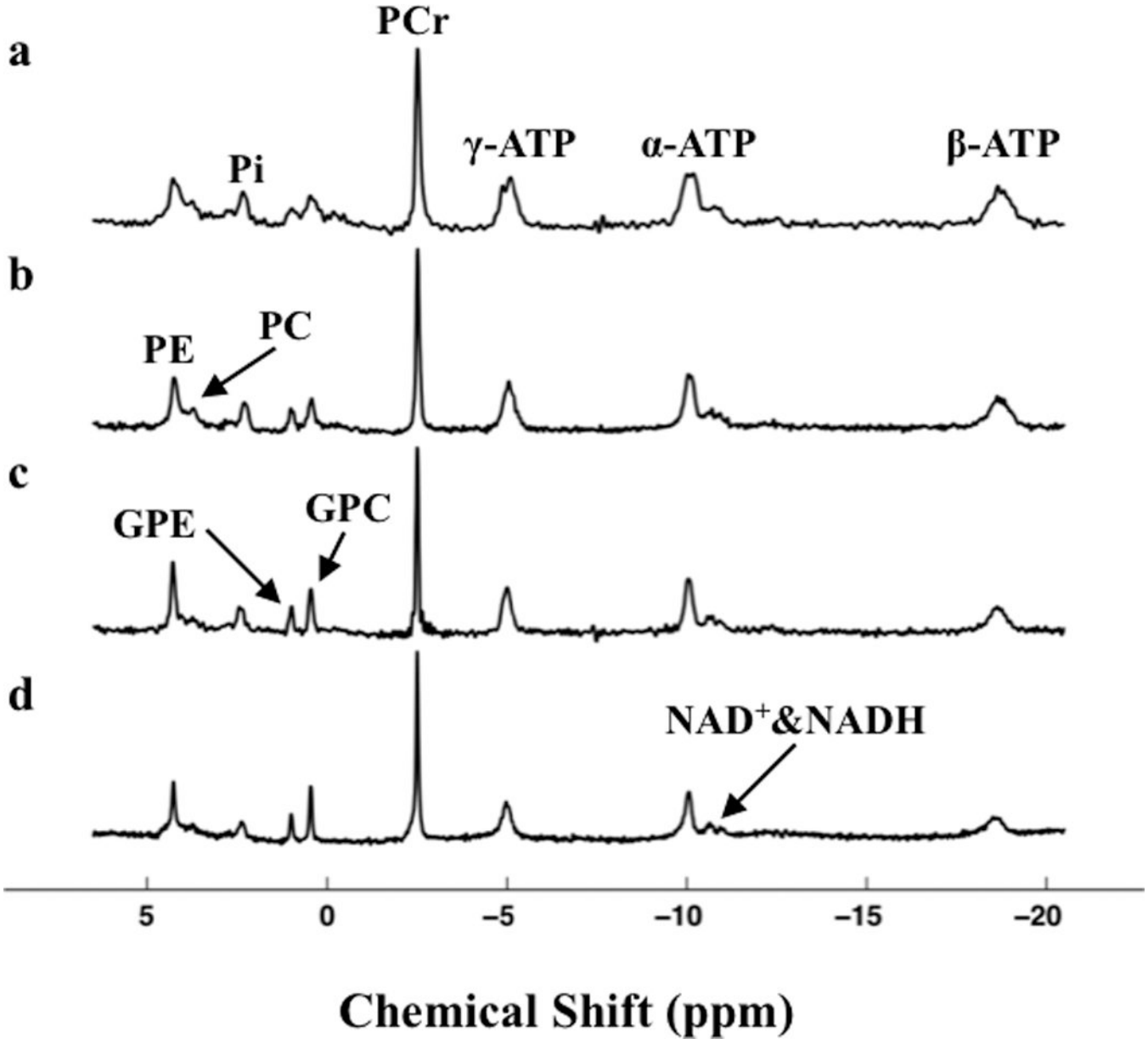

Figure 1.

In vivo ^{31}P spectra of visual cortex acquired at (**a**) 4 T (TR=6s, NT=192) and (**b**) 7 T (TR=16s, NT=128) from human brains, and at (**c**) 9.4 T (TR=16s, NT=64) and (**d**) 16.4 T (TR=5s, NT=40) from cat brains and processed without any line broadening (LB=0). PE: phosphoethanolamine; PC: phosphocholine; GPE: glycerophosphoethanolamine; GPC: glycerophosphocholine; NAD^+ & NADH: oxidized and reduced forms of nicotinamide adenine dinucleotide.

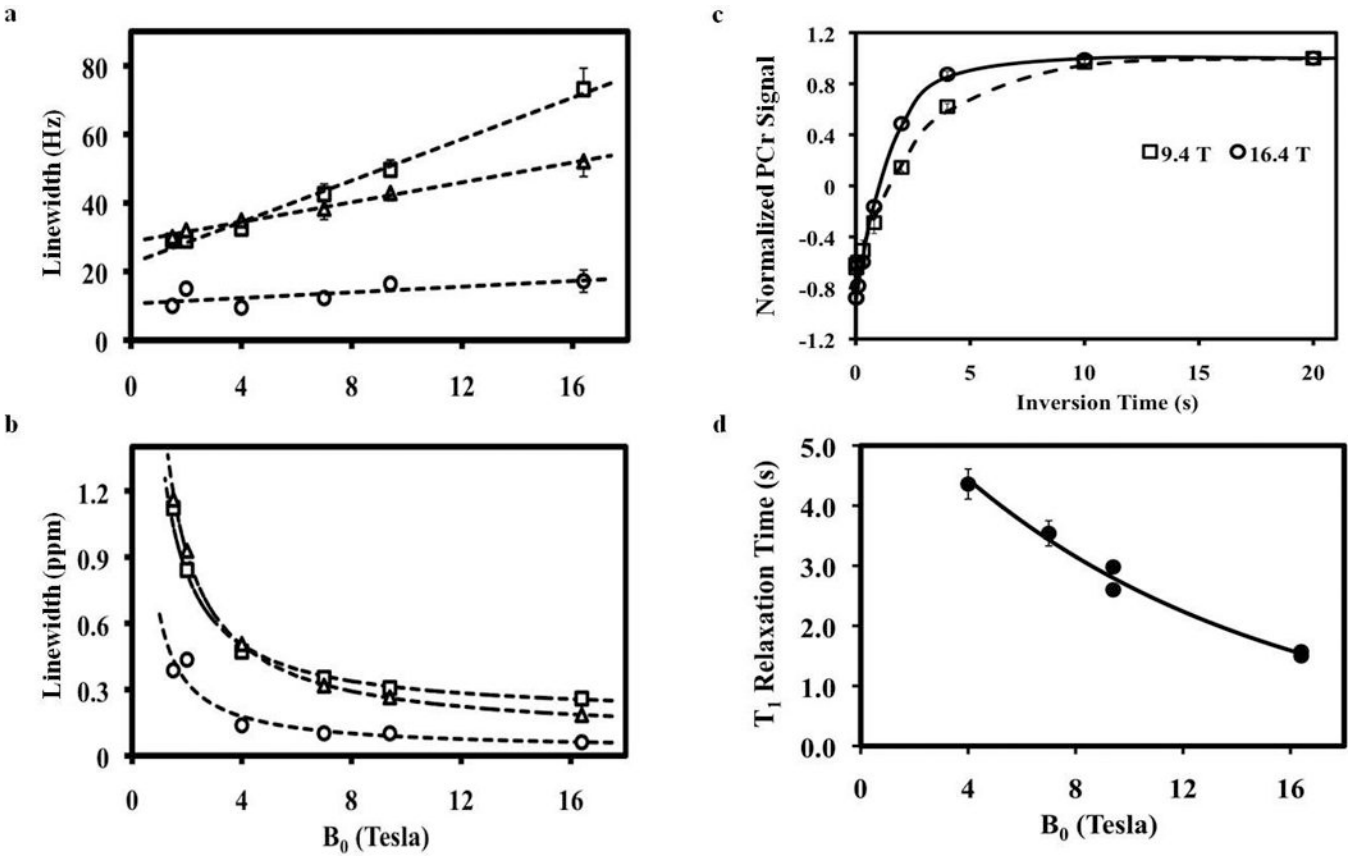

Figure 2.

Field dependences of PCr (○), γ-ATP (□) and α-ATP (**Δ**) linewidths display in the unit of Hz (**a**) and ppm (**b**). Dashed lines demonstrate the regression curves and correlations between linewidths and B_0. The data of 1.5 T and 2 T were taken from the literature (21). (**c**) ^{31}P T_1 relaxation time measurements of PCr in the rat brains at 9.4 T and 16.4 T. Solid and dashed lines are the exponential fittings of the T_1 data at 16.4 T and 9.4 T, respectively. (T_1 = 2.95 ± 0.11 s for 9.4 T and 1.56 ± 0.05 s for 16.4 T) (**d**) Field dependence of PCr T_1. Solid line indicates the regression curve and correlation between PCr T_1 and B_0.

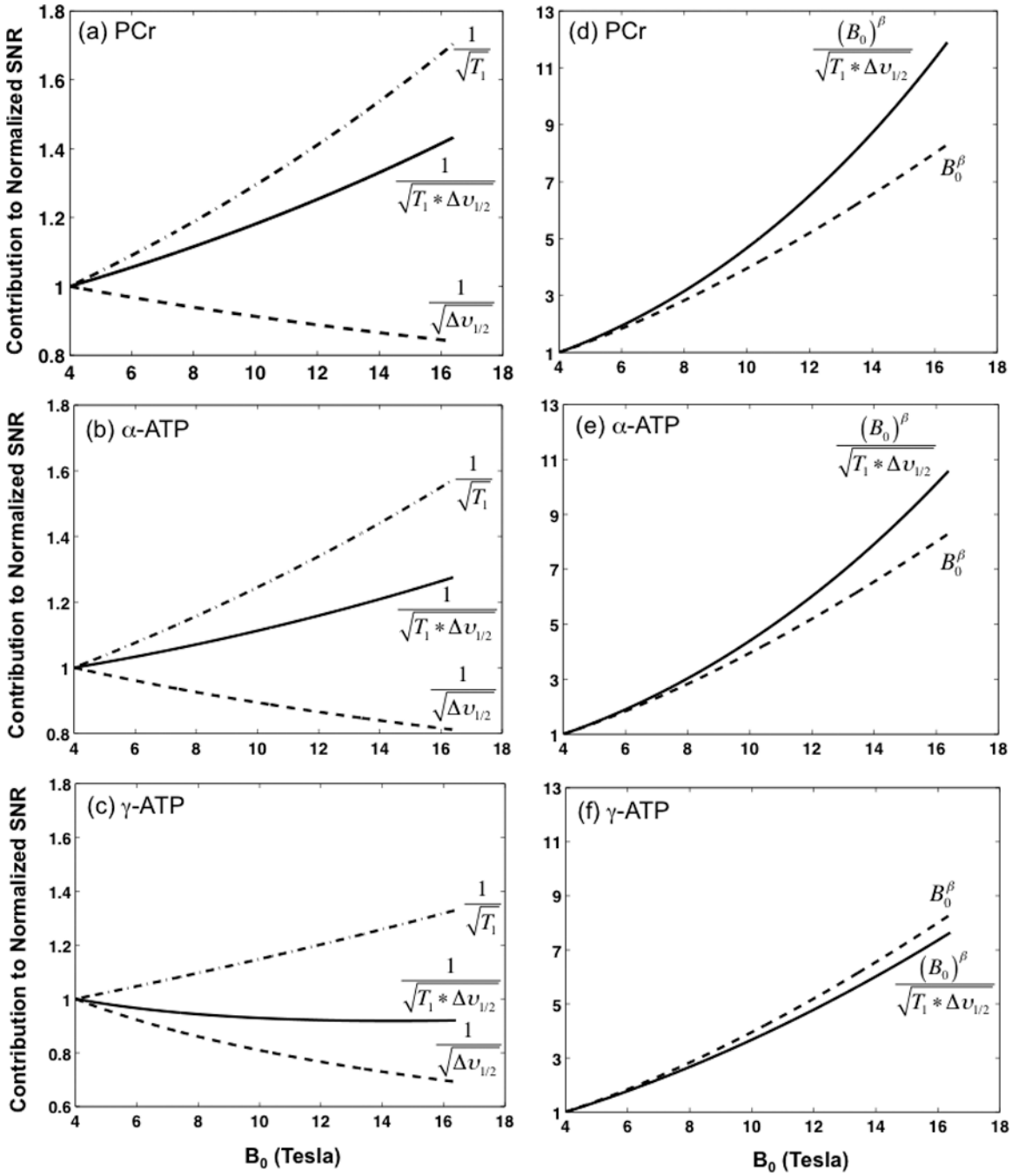

Figure 3.

Field dependences of relative contributions from T_1 and $\Delta\nu_{1/2}$ (**a**, **b** and **c**), and from T_1, $\Delta\nu_{1/2}$ and B_0 (**d**, **e** and **f**) to the brain ^{31}P SNR (normalized to 4 T) determined for the PCr (**a** and **d**), α-ATP (**b** and **e**), and γ-ATP (**c** and **f**) resonances, respectively.

Table 1

Summary of field-dependent parameters for the sensitivity comparison study of rat brain between 9.4 T and 16.4 T using the single-pulse-acquisition approach

B_0	Rat Brain SNR (N=5) (8 averages)	T_1 (S), N=4	$\Delta\nu_{1/2}$ (Hz), N=5	Coil Q	G (TR/T_1)	$(1-E_2^2)^{1/2}$
16.4 T	80.2 ± 4.7	1.56 ± 0.05	32.8 ± 1.62	353.5	0.56	1
9.4 T	46.1 ± 6.0	2.95 ± 0.11	21.8 ± 0.9	405	0.74	1
Ratio	1.74	0.529	1.505	0.873	0.757	1

For calculation of the G and E_2^2 factors, *at*=0.064 s and TR=10 s were used for both field strengths. Coil Q values were measured experimentally with rat brain loading.